ISPRS Journal of Photogrammetry and Remote Sensing 101 (2015) 102–109

Contents lists available at ScienceDirect

ISPRS Journal of Photogrammetry and Remote Sensing

journal homepage: www.elsevier.com/locate/isprsjprs

Potentials and limitations of SAR image simulators – A comparative study of three simulation approaches

Timo Balz [a,*], Horst Hammer [b], Stefan Auer [c]

[a] State Key Laboratory of Information Engineering in Surveying, Mapping and Remote Sensing, Wuhan University, 129 Luoyu Road, Wuhan 430079, China
[b] Fraunhofer Institute of Optronics, System Technologies and Image Exploitation, Fraunhofer Society, 76275 Ettlingen, Germany
[c] Chair of Remote Sensing Technology, Technische Universität München, 80333 München, Germany

ARTICLE INFO

Article history:
Received 22 January 2014
Received in revised form 11 October 2014
Accepted 5 December 2014

Keywords:
SAR
Simulation
Rasterization
Ray tracing
Modeling

ABSTRACT

Various applications, like for instance algorithm design, mission planning, geo-referencing, change detection, Automatic Target Recognition (ATR) or SAR data analysis, rely on simulated synthetic aperture radar (SAR) images. However, there are different SAR simulation techniques with different advantages and disadvantages. Depending on the needs of a certain application, a suitable SAR simulation technique has to be used. This paper compares three SAR image simulation approaches, RaySAR, CohRaS®, and SARViz, showing their similarities and differences. RaySAR and CohRaS® are two ray tracing based SAR image simulators. RaySAR is based on the open-source software POV-Ray, while CohRaS® is developed as SAR simulator from scratch. The third simulator, SARViz, is a real-time SAR simulator based on the rasterization approach. The geometrical features of the three simulators are compared and the differences and different applications are analyzed.

1. Introduction

The simulation of synthetic aperture radar (SAR) data has many applications in radar remote sensing, for example in sensor and algorithm design, mission planning, geo-referencing, SAR data analysis and interpretation, etc. This wide variety of applications leads to a variety of SAR simulation approaches, each fitting best for specific objectives and preconditions. However, no simulator is suitable for all scenarios or applications.

According to Franceschetti and Migliaccio (1995) two main types of SAR simulation systems can be distinguished: SAR image simulators, which directly provide focused images, and SAR raw signal simulators, which deliver SAR raw data for processing. In this context, different signal reflection models may be utilized. Scattering can for example be simulated using the Kirchhoff physical optics (PO) (see Ulaby et al., 1986), the geometrical optics (GO) approximations (Franceschetti et al., 2003), the integral equation method (IEM) (Xu and Jin, 2006), a more simplified approach related to the Phong shading model (Brunner et al., 2011), or combinations of these.

In our work, we focus on SAR image simulators for applications in urban areas. Therefore, we will use the term SAR simulators as short form for SAR image simulators in the remaining text. SAR simulators assist radar remote sensing in urban areas in different ways. Mission planning is, for example, one important application (Gelautz et al., 1998). Another important field is the assistance of SAR image interpretation in complex urban areas, where SAR simulators help to identify the origin of backscattering contributions (Brunner et al., 2011) (Auer, 2011). Furthermore, SAR simulators can be used to create synthetic input data for the training of classifiers, and finally, the 3D localization capability of interferometric SAR algorithms such as persistent scatterer interferometry or SAR tomography can be analyzed (Auer et al., 2011a). Different case studies on buildings reveal that the scene geometry is the major issue for the distribution and appearance of SAR image signatures, e.g. (Auer, 2011; Auer et al., 2011b). Accordingly, SAR simulators have to be capable to consider all scene details. For instance, facade details such as window corners or balcony elements must not be neglected, e.g., for rendering complex analytical reflection models applicable.

In this study, we compare three recent SAR simulators fulfilling this requirement, RaySAR (Auer, 2011), CohRaS® (Hammer and Schulz, 2009), and SARViz (Balz and Stilla, 2009), which can be classified as integrated SAR image simulators. That is, the simulators do not provide raw signal data but directly simulate SAR images. They have been developed for the simulation of high-resolution SAR

* Corresponding author.

http://dx.doi.org/10.1016/j.isprsjprs.2014.12.008

data, comparable to the data from airborne or spaceborne SAR sensors. For the latter case, the focus is on the analysis of man-made objects in high-resolution SAR data. In this context, the main difficulty is to interpret or predict the geometric shape of objects, because the imaging of dense urban areas is heavily affected by distortion effects (Stilla, 2007). An overview of the simulator properties is given in Table 1.

Overall, the paper addresses three new aspects. First, a detailed comparison of three simulation concepts, between two different ray tracing and one rasterization approach, is provided. Second, simulations that use basic object models as a benchmark for testing future simulation systems are conducted to support the comparison. Finally, the paper may be helpful as a guide for the planning of future simulation concepts focused on detailed object geometries.

This paper is organized as follows. Section 2 gives a brief introduction of the simulation techniques. Thereafter, geometric properties of the simulators are compared in two case studies (building model, silo model) in Section 3. The paper concludes with advantages and disadvantages of the compared simulators in Section 4, in combination with the suggestion of design specifications for new simulators depending on their proposed applications.

2. SAR simulators

2.1. RaySAR

RaySAR (Auer, 2011; Auer et al., 2010) is a 3D SAR simulator based on ray tracing methods, implying an enhanced version of the open-source software POV-Ray for simulating radar signals in 3D, i.e. azimuth, range, and elevation. As a result, the simulated signal contributions can be compared to object geometries reconstructed by interferometric SAR methods, e.g. SAR tomography (TomoSAR) (Zhu and Bamler, 2010) or persistent scatterer interferometry (PSI) (Gernhardt et al., 2010). The focus of the simulation concept is on local urban scenes imaged by very high-resolution (VHR) SAR sensors and on the geometric correctness of simulated signals. Random scattering is neglected as the main goal is to identify and understand deterministic reflection effects occurring at individual man-made objects. A combination of two basic reflection models is used to simulate the spatial distribution of diffuse and specular reflection signals. The results of different case studies related to the interpretation of TerraSAR-X (TSX) data are summarized in (Auer, 2011).

2.2. CohRaS®

CohRaS® (Coherent Raytracing SAR Simulator) (Hammer and Schulz, 2009. 2011), is a SAR simulator based on ray tracing methods. The ray tracer itself is based on the concept developed by Amananatides and Woo (1987). This simulator is intended mainly for the simulation of small scenes with high resolution for creating training data for classifiers and sample data for the training of image analysts. The only restriction imposed on the geometry of the 3D model, is that all polygons need to be convex. The focus is set on the fast calculation of many small images, as this is needed for classification. Also, in order to be able to compare the simulated image chips in an automated process to real SAR images of the objects, it is necessary to simulate the radiometry of the objects if possible, and to have a material model that can easily be adapted to different materials found in the real images. In the CohRaS® simulator this is achieved using a twofold model: First of all, diffuse reflection is modeled by a Lambertian approach, i.e.

$$\sigma_{back,diff} = \sigma_0 \cdot \cos^2(\theta)$$

where σ_0 is a theoretical backscattering coefficient that could be measured in the total absence of any specular reflection and when looking perpendicular to the surface, and θ is the local incidence angle of the wave on the surface. Specular reflection is modeled differently:

$$\sigma_{sp} = \sigma_{max} \cdot \cos^a(\theta) \cdot \cos^b(\gamma)$$

where σ_{max} is the maximum expected backscattering coefficient when looking at the surface perpendicularly, θ, as above, is the local incidence angle, γ is the angle between the direction to the observer and the true specular direction, and a and b are free integer parameters to tune the materials. The second cosine term accounts for the fact that most materials show quite high energies not only in the true specular direction but rather in a small cone around this direction. In order to be consistent, the maximum of $\sigma_{back,diff}$ and σ_{sp} is used.

2.3. SARViz

SARViz (Balz and Stilla, 2009) is a real-time SAR image simulation system. The preface "real-time" is used in the computer graphics sense, which, in our case, means more than 20 simulations or frames per second. The size of each frame is typically 1024×768 pixels. SARViz uses the rasterization approach implemented on Graphics Processing Units (GPU), which allows very fast simulations, but has certain limitations regarding to the geometric and the radiometric accuracy. For example, rasterization does not allow simulating multiple bounces, because the path of the waves throughout the scene is not known. With the increased flexibility and programmability of modern GPUs, a GPU based hybrid ray tracing approach was implemented in SARViz for double bounce simulation (Balz and Stilla, 2009).

3. Potentials and limitations of the presented SAR simulation approaches

Depending on the intended application, a SAR simulation system has to fulfill certain requirements, but also simplifications need to be made in order to achieve acceptable calculation times. A simple example would be SAR simulators used for visibility analysis in mission planning. To this end, a simple shadow and layover

Table 1
Properties of the simulators.

	RaySAR	CohRaS®	SARViz
Processing type	Ray tracing	Ray tracing	Rasterization
Radiometric processing	Derived from Phong shading (see Auer, 2011)	See Section 2.2 or (Hammer and Schulz, 2009)	Derived from Phong shading (see Balz and Stilla, 2009)
Speckle	No speckle support	Random scatterer positioning	Random multiplicative speckle
InSAR support	No	Yes	No
Developed with	POV-Ray	CPU with vectorization	GPU via DirectX
Applications	PS-InSAR analysis, automated change detection	Target classification	Real-time simulation

analysis is sufficient. The geometrical correctness and the speed of the simulation should be high, whereas no backscattering model needs to be implemented at all. On the other hand, simulators used to assist target detection or classification typically require a sophisticated backscattering model supporting realistic polarized backscattering behavior.

The three SAR image simulation systems compared in our study are focused on the geometrical correctness of the simulation. They do not aim at modeling the stepwise data acquisition along the synthetic aperture. Therefore, there is no loss of resolution or amplitude if an object is only partially visible all along the synthetic aperture. This limitation is present for all SAR image simulation systems, because the simulation of the synthetic aperture requires the generation of raw data. Also because of this, neither SARViz, nor CohRaS® or RaySAR enables the correct simulation of moving targets. However, the direct simulation of image data and the acceptance of simplified reflection models enable the simulation of very detailed object geometries (single and multi-body scenes). This potential is crucial for understanding the appearance of dominant signatures in high resolution SAR images as the corresponding signal responses are often related to structural elements of small size, e.g. corners at balconies/windows or roof structures in case of urban buildings. In this regard, the potentials of RaySAR, CohRaS® and SARViz have already been reported (see Section 2).

For comparing the simulator properties, the potentials and limitations of the different SAR simulation concepts can be better explained and understood, when interpreting simulated images of basic object models. To this end, two simple 3D models have been chosen: A building model represented by a cube with inserted windows, and a silo model, with a roof railing on top, whose curved surface is approximated by flat patches. Using the same model files and imaging geometries, the simulated images are cross-comparable from a geometric point of view. Since the radiometric models are too different to enable a direct comparison, only the generated reflectivity maps are shown. Both object models, i.e. building and silo, are available for download for testing available simulation tools or SAR simulators under development (link: http://insar.l-mars.whu.edu.cn/models).

The building model in Fig. 1(a) has been chosen as it may resemble basic characteristics pertinent to real urban buildings. It is surrounded by flat terrain and its basic form is composed by flat surfaces. Moreover, it contains regular shapes (window corners) which, in real urban scenes, are often related to dominating point signatures in SAR images. The building, whose dimensions are $10 \times 10 \times 5$ m, is rotated with respect to the line-of-sight of the SAR sensor (rotation angle: 50°) and is assigned with surface parameters (dominant specular reflections, diffuse backscattering enabled for visualizing the building extent). Fig. 1 shows the resulting images provided by SARViz, RaySAR, and CohRaS®. They are simulated with a spatial resolution of 0.8 m in azimuth and range, and with a signal incidence angle of 40°. All three simulators are getting similar results for the basic features of the building. However, specific properties of the simulation methods can be distinguished.

3.1. Building model

SARViz is oversampling each scene for anti-aliasing and a better visual impression of the simulated image. As described above, SARViz can only simulate single and double bounce reflections and does only support incoherent summation (i.e. signal phase is not considered). This is the reason for several missing features in the simulated image for the building model (see Fig. 1(a) and (b)) compared to RaySAR and CohRaS®, especially the missing triple bounce reflections of the windows and window edges is obvious. The double bounce reflection at the building edge is also comparably weak. This is a result of the image based double bounce simulation technique used, which seems to underestimate the double bounce reflection in this case.

RaySAR provides images in two steps. First, the modeled scene is sampled by an enhanced version of the POV-Ray ray tracer. Thereafter, the detected signal contributions are imposed with a pixel grid and summed in order to derive the final image. The summation can be conducted coherently considering the signal amplitude and phase (distance information given by the ray tracer), or incoherently by simply summing the intensities within the resolution cell. Besides a reflectivity map containing all amplitude information, the simulated signal contributions are assigned to separate image layers and are classified into specular and diffuse reflections. A detailed description of the use of this additional simulation data is beyond the scope of this paper and is given by Auer (2011).

Fig. 1(c) shows the result of the incoherent summation of signal amplitudes for the building model. The basic geometric shape of the "building signal" equals the shape simulated by SARViz. Nonetheless, a closer look reveals differences. First, the double bounce lines are longer ("double bounce tails"), which is related to the consideration of processing effects in azimuth direction (see Auer, 2011) for a detailed explanation). Second, the backscattering from windows is mainly represented by point signatures related to triple reflections at corners. Finally, signatures are distinguishable in the shadow area of the building. In more detail, diffuse signals related to fourfold signal reflections form linear features and are overestimated due to incoherent summation. Fivefold reflections are of type "specular" and yield six dominant point signatures. The pattern-like representation of ground parts occurs due to the imposing of a raster onto discretely simulated signal contributions. As the main focus of RaySAR is on point signatures, no anti-aliasing methods have been implemented yet.

The result of the coherent summation can be seen in Fig. 1(d). The main difference with respect to Fig. 1(c) is the loss of amplitude for the layover area and for the double bounce tails, which are almost negligible. The reason is that the variation of phase angles of diffuse signals is considered during the image formation step. Signatures in reflectivity maps with coherently summed signal contributions can be better cross-compared to real SAR images. However, for orientation purposes, surface parameters have to be manipulated if the extent of diffuse signatures is to be clearly seen in the simulated image. As expected, the strength of point signatures related to specular reflections equals the result of the incoherent simulation (constant phase angle).

The dependence of the signal strength on the geometric size of corner reflectors is represented correctly (Auer, 2011). Doubling the size of a corner reflector also doubles the strength of the simulated amplitude. In contrast, the simulation of diffuse signals is based on simple reflection models (Lambertian or angular dependent scattering). As a consequence, the modeling of the proportion between diffuse and specular signal reflections is moderate in general. However, at present, this limitation is accepted as the focus of RaySAR is on the analysis of specular multiple reflections, and an overestimation of diffuse signals may be welcome for orientation purposes (e.g. for selecting pixels of interest).

The CohRaS® image formation is performed using ray tracing on the 3D geometry model. The number of rays that are traced can be set by the user and is an important parameter that influences both the quality of the simulation and the calculation time. For all polygons visible to the sensor, direct returns are calculated. For each of these, also the specular path is calculated, if the maximum number of specular reflections has not been reached. If the specular reflected ray hits another part of the scene, both the direct return to the sensor and further specular reflections are calculated.

To simulate speckle, a fixed number of point scatterers is placed in a random process on each of the polygons of the 3D scene

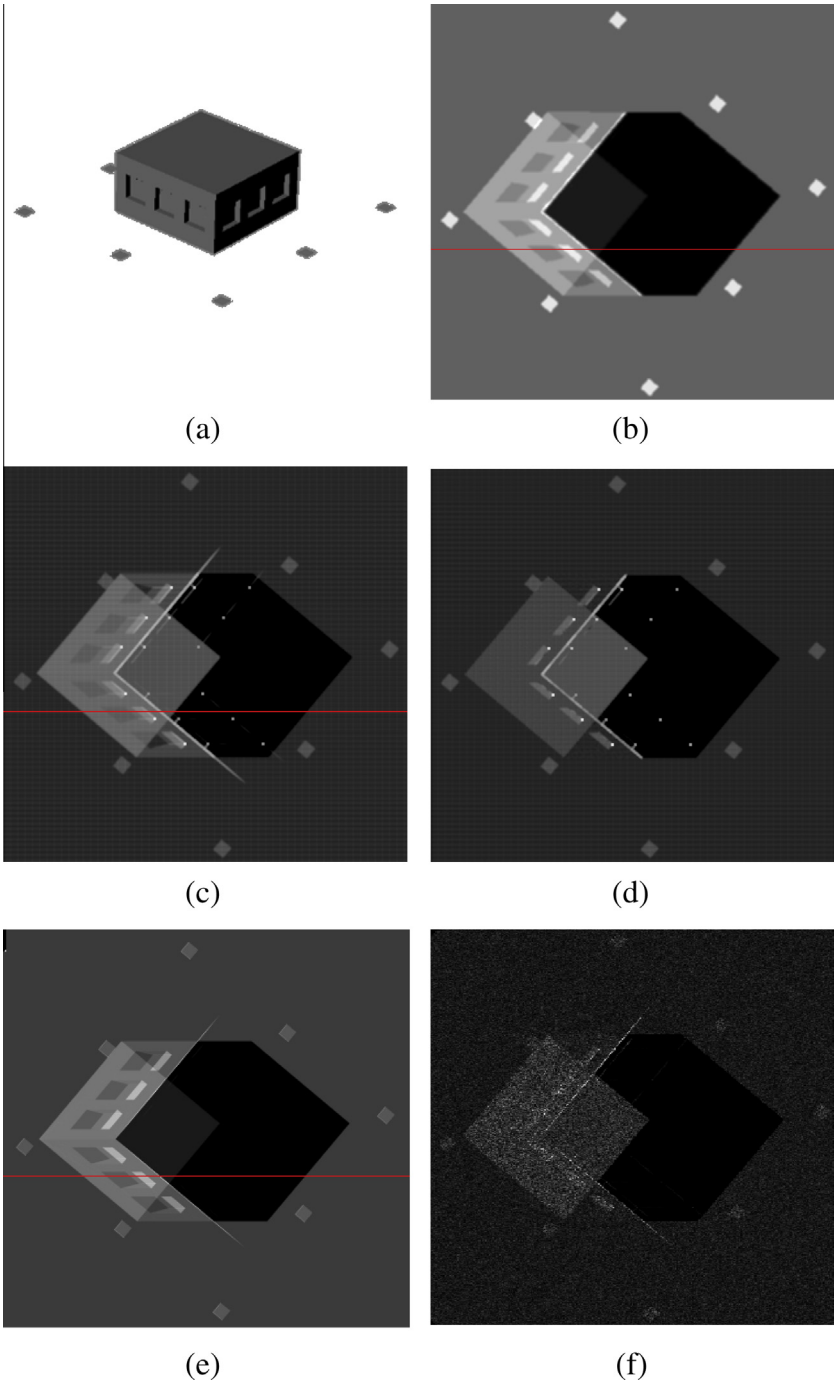

Fig. 1. SAR simulation of a simple building model. (a) 3D building model, including eight square patches for co-registration, (b) SARViz simulation, (c) RaySAR simulation, incoherent summation (separate reflection levels: 1–5, i.e. direct backscattering, double reflection, triple reflection, etc.), (d) RaySAR simulation, coherent summation (1–5), (e) CohRaS® simulation, one point scatterer per resolution cell (no speckle), incoherent summation (1–5), and (f) CohRaS® simulation, coherent summation, 6 point scatterers per resolution cell (speckle simulation) (1–5). The red line marks the position of the profile shown in Fig. 2. (For interpretation of the references to color in this figure legend, the reader is referred to the web version of this article.).

belonging to a certain resolution cell. If visible to the sensor, the returns of all of these point scatterers are coherently added to get the overall signal of the polygon.

The result of this process, as is the case for RaySAR, is a reflectivity map. The reflectivity map for the building model is shown in Fig. 1(f) using six point scatterers per polygon and resolution cell. In order to be comparable with the results of SARViz and the incoherent result of RaySAR shown in Fig. 1(c), the building model has also been simulated with only one point scatterer per polygon and resolution cell and incoherent summation (see Fig. 1(e)).

The results obtained with RaySAR and CohRaS® for incoherent summation are quite similar, which is to be expected considering the very similar approach based on ray tracing used in these two simulators. Most of the differences come from a slightly different modeling of the materials, that leads e.g. to a brighter dihedral corner reflection line in CohRaS® than in RaySAR.

Summing up this first simulation experiment, all three simulators are able to perform the basic geometric simulations producing the same layover and shadow areas and the same imaging geometry. Differences are mainly due to the missing multiple bounces in SARViz and due to the different modeling of the material properties, which will be discussed further in the next section.

The modeling of the materials is different for the three simulators. This is because in the simulation process, different assumptions are made that model the creation of the processed SAR image without creating raw data. So for each of the simulators, the materials model is adapted to these assumptions so that the simulated images resemble corresponding real images as closely as possible.

The lack of global illumination in the three presented simulators also reduces the accuracy of the simulation and may lead to an overestimation of the intensity of specular reflections, especially in multi-bounce scenarios. These do not match the assumptions made in SAR raw data processing and thus only appear as bright spots in processed SAR images if they are stable over large parts of the synthetic aperture. In the simplified ray tracing approach, bright multi-bounce spots may occur simply by chance, because for the single ping considered the geometry may lead to direct specular returns whereas this may not be true over the whole aperture. The diffuse reflection of objects is not simulated accurately, because diffusely scattering objects are scattering their energy in all directions, whereas in the presented simulations only the part of the energy scattered back to the sensor (see e.g. the evaluation in Auer, 2011) and the part scattered in the specular direction are considered, in order to save calculation time. Brunner et al. (2011) implemented a more complete solution for global illumination within the incident field.

For a detailed comparison of the image geometry and radiometry, we define a reflection profile in range direction. The backscattering models and surface parameters used by the three simulators are different. Moreover, the dynamic range of signal amplitudes is different. Hence, a direct comparison of the backscattering profiles is not reasonable. However, for distinguishing and discussing systematic effects pertinent to the simulated images, we use normalized backscattering profiles. For each SAR image profile, the backscattering results are normalized linearly between 0.0 for the lowest backscattering in that profile and 1.0 for the highest backscattering.

Using normalized profiles, we still do not expect to see identical values all along the profile because of the different backscattering models and surface parameters. However, if the geometry is correct, changes should appear at the same positions. For instance, we can also expect similar peaks and valleys and comparable backscattering patterns throughout the profiles. Fig. 2 shows the backscattering profiles of the simulation results along the profile marked red in Fig. 1. Beforehand, the simulated images have been co-registered using the eight planar patches surrounding the building (see Fig. 1(a)), whose surface roughness is significantly higher than the roughness of the ground plane.

The normalized profiles shown in Fig. 2 show the high geometrical similarity between the simulators. The three different simulation techniques are all able to simulate the basic geometrical properties of a SAR image. However, the radiometric results are different, due to the different techniques used in the simulators.

The profiles are normalized, so that the strongest scatterer, which is double bounce scattering at the building edge, is normalized to 1.0. Therefore, we can see that RaySAR shows the highest radiometric dynamics, SARViz shows the lowest dynamics and CohRaS® is somewhat in between. The backscattering from the window frame, the second highest peak in the profile, is also estimated to be quite strong in the CohRaS® simulation compared to the surrounding areas, but comparable in strength to the double bounce scattering. RaySAR is estimating the difference between the double bounce and the window frame relatively higher and in SARViz both are even identical.

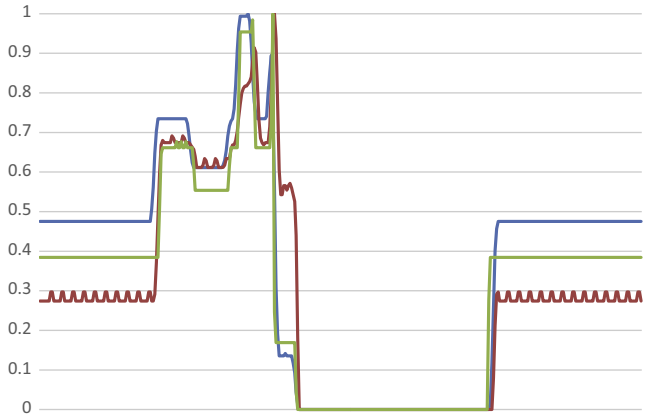

Fig. 2. Profile of the normalized backscattering values along the red lines in Fig. 1; SARViz (blue), RaySAR with incoherent summation (red), and CohRaS® using only one scatterer per cell and incoherent summation (green). (For interpretation of the references to color in this figure legend, the reader is referred to the web version of this article.).

In comparison to the ray tracing based simulators, SARViz is clearly underestimating the strength of the double bounce. This is most likely caused by the image-based way SARViz is using for calculating double bouncing, which can lead to an underestimation of the double bounce intensity.

Considering the different approaches taken for the modeling of the materials, the similarities of the three curves are striking: while the absolute values may differ and the balance between specular and direct reflection intensities may differ a bit, the profiles are in very good accordance, i.e. changes occur in the same place for all simulators. In addition, the shape of the curves is very similar, even though the backscattering models and the surface parameters are defined individually for each simulator. What is apparent in the RaySAR results is the ripple structure caused by aliasing. This can be avoided by oversampling the simulated image, which is done by CohRaS® and SARViz.

3.2. Silo model

The silo model has been selected as it contains a curved surface (see Fig. 3(a)) and a railing at the rooftop. A closer look reveals that the curvature is represented by narrow patches, which is common for 3D object models. CohRaS® only supports geometries made up of convex polygons; SARViz only supports models consisting of triangles. RaySAR does support the simulation of round surfaces if they are defined analytically in the POV-Ray editor. For SAR image simulation systems, the lack of support for curved surfaces is often acceptable, because the synthetic aperture is not simulated. For raw data simulators simulating the formation of the synthetic aperture along azimuth, the ability to simulate curves is important, because it allows to correctly simulate the backscattering contributions of round objects. Using the silo model for testing, systematic simulation effects related to the curvature approximation, especially direct backscattering and double reflections, can be analyzed. Eventually, the appearance of simulated edges can be seen for pure geometrical simulation, i.e. if physical effects at edges are neglected.

Fig. 3(b)–(f) shows the simulated reflectivity maps for the silo model. In Fig. 3(b), we see an interesting effect: the edge of the lid of the tank is backscattering in the SARViz simulation. This error is caused by shadow mapping, which is a technique used by SARViz

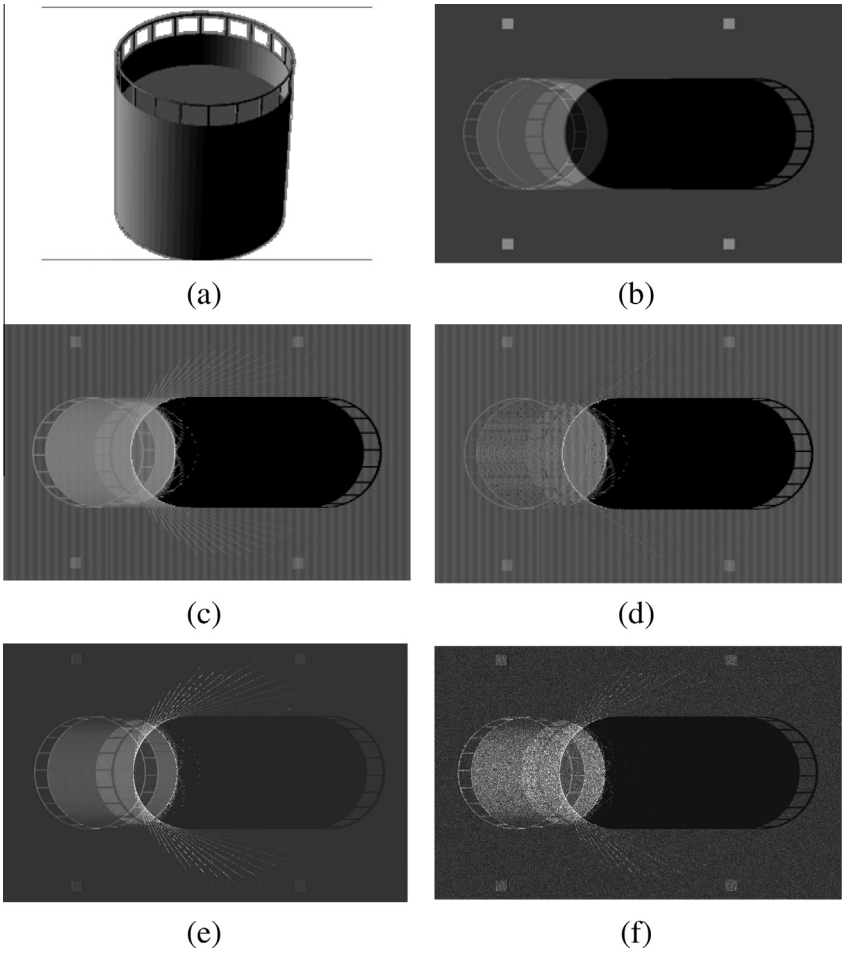

Fig. 3. SAR simulation of a silo model. (a) 3D silo model. (b) SARViz simulation, (c) RaySAR simulation (reflection levels: 1–3, incoherent summation), (d) RaySAR simulation with coherent summation, (e) CohRaS® simulation, one point scatterer per resolution cell (1–3), and (f) CohRaS® simulation, 6 point scatterers per resolution cell, coherent summation (1–3).

to calculate occlusions. Shadow mapping is image based, very fast, but with a limited precision, which leads to an erroneous simulated backscattering from the lid, because SARViz is assuming that parts of the lid are visible.

In the RaySAR simulation in Fig. 3(c), the polygon description of the silo model yields two groups of faint diffuse double bounce lines next to the upper and lower end of the shadow area. For a real curved silo, these fields are expected to be smeared for two reasons. First, the intensity of diffuse signals is overestimated for reflection levels larger than 1 if scene objects are not of Lambertian nature. Second, both the polygons approximating the curved shape as well as the discrete sampling by the ray tracer trigger the appearance of faint double bounce lines, whose strength weakens with coherent summation (see Fig. 3(d)). The radiometric limitations are acceptable as the focus is on the geometry of the SAR image, i.e. RaySAR represents the geometrical extent of the phenomenon.

The signature of the silo obtained with CohRaS® is shown in Fig. 3(e) for the incoherent simulation with one point scatterer per polygon fragment. This signature is quite similar to the one obtained with RaySAR. Here, the fan of double bounce lines due to the discrete polygonal representation of the round silo is clearly visible. The most striking difference between the RaySAR and CohRaS® simulations is the consideration of local incidence angle in the modeling of the direct reflections in CohRaS®. This leads to the diminishing returns from the wall of the silo visible in Fig. 3(e) and (f). Again, the dihedral corner lines become weaker with coherent simulation, however they do not completely disappear.

The comparison between the RaySAR/CohRaS® results and the simulation result obtained by SARViz is best performed using the incoherent summation with only one point scatterer per voxel. From these simulations, it again becomes clear that all three simulators feature the correct geometry, although the shadow mapping technique in SARViz leads to a rather large error. Thus, all three can be used for the identification of layover and shadow areas in SAR images.

3.3. Eiffel tower

The model of the Eiffel tower was chosen to demonstrate the ability of the different SAR simulation tools to handle geometries that are more complex. In addition, a real SAR image recorded by TSX was available, so that the simulated signatures could be compared to this image to evaluate the performance of the simulators. The simulation parameters were adapted to the TSX spotlight imaging mode with a pixel spacing of 0.43×0.40 m in azimuth and range, an incidence angle of 34.7°, and a heading angle of 346.36°. A screenshot of the model is shown in Fig. 4, the comparison of the simulation results with a TSX image are presented in Fig. 5.

Fig. 4. 3D model of the Eiffel tower.

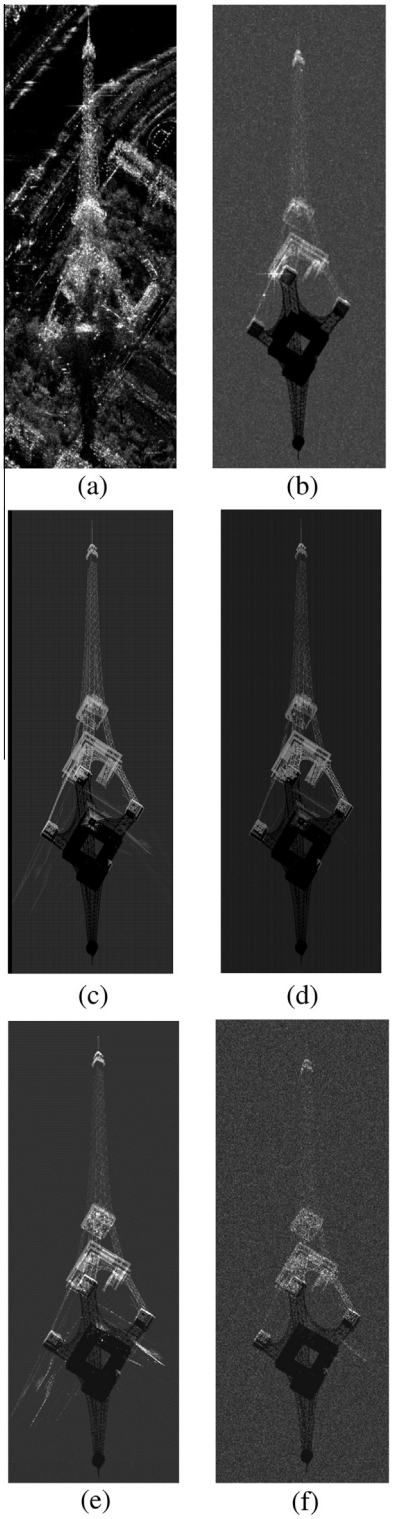

Fig. 5. SAR simulations of the Eiffel tower. (a) TSX image captured in spotlight mode (image taken from Auer et al., 2010), (b) SARViz simulation, (c) RaySAR simulation (reflection levels: 1–5, incoherent summation), (d) RaySAR simulation with coherent summation, (e) CohRaS® simulation with only one point scatterer per resolution cell (reflection levels: 1–3), and (f) CohRaS® simulation with six point scatterers per resolution cell and coherent summation (reflection levels: 1–3).

The simulation of the geometrical features works again quite well and for all three simulators. The amplitude is different in different simulations, mainly because of different handling of materials and a lack of a common material model, which would allow a better comparison of the simulations. SARViz is lacking the capability to simulate triple bouncing, which explains the missing ghost-scatterings in Fig. 5(b). Nonetheless, the simulated image of SARViz, considering the spatial resolution of the TSX sensor, enables to confirm and interpret the visual appearance of the tower in the SAR image.

As SARViz does not follow any rays throughout the scene, it is unaware of distances and travel times of the signal, which makes it impossible to simulate the complex signal and use the SARViz approach for the simulation of interferometric scenes. Complementary to the SARViz result, the simulated images of RaySAR and CohRaS® focus on varying the pixel spacing of reflectivity maps, which are independent of the spatial resolution of the SAR sensor. The maps provided by RaySAR (coherent, coherent) are adapted to the pixel spacing of the TSX image (Fig. 5(c) and (d)).

Compared to the SAR image, the tower structures are better distinguishable as only the position of signal phase centers in the azimuth-range plane is represented (i.e. the peak position of the 2D signal response function). Further increasing the visibility of details, the reflectivity maps simulated by CohRaS® (Fig. 5(e) and (f)) are based on pixel spacing values of 5 cm, indicating the potential of ray tracing methods for simulating future SAR systems with increased spatial resolutions.

4. Discussion and conclusions

SAR images can be simulated using different simulation concepts. In this paper, three different SAR image simulators (SARViz, CohRaS®, RaySAR) are compared, all capable of simulating the basic SAR geometry correctly. For simple geometric simulations, for example in the context of layover and shadow analysis, simple and fast solutions such as SARViz are preferable. However, if multi-bounce simulation is required for detailed object geometries, a ray tracing approach is recommended, because the rasterization approach does not support multi-bouncing.

For simulating the amplitude of the backscattering, the simulators follow slightly different concepts. Comparing these concepts is very difficult, given that each method is based on different parameters and material descriptions. For instance, each simulator has its own set of parameters, typically describing the backscattering strength as well as the roughness of the surface. In connection with the approximations made during the image creation process, the simulators provide images best suited for the respective field of application.

In summary, most applications of SAR image simulators will work best with an approach based on ray tracing. Ray tracing is also rather easy to implement, although it is not necessarily computational efficient. Implementations can be based on available software packages or libraries, which further reduce the development time. Only few applications need the real-time capability of rasterization based SAR simulation approaches. With the increase in parallel processing power and the very parallel nature of ray tracing, fast and near real-time SAR simulations using ray tracing will also be possible in the near future, which makes the development of SAR simulators based on ray tracing even more interesting.

Acknowledgements

Parts of this work are financially supported by the National Natural Science Foundation of China (Grant No. 61331016 and 41174120) and by the Deutsche Forschungsgemeinschaft (DFG), Project VHR-SAR (BA 2033/3-1).

References

Amananatides, J., Woo, A., 1987. A Fast Voxel Traversal Algorithm for Ray Tracing. In: Proc. Eurographics '87. Amsterdam, pp. 3–10.

Auer, S., 2011. 3D synthetic aperture radar simulation for interpreting complex urban reflection scenarios. Deutsche Geodätische Kommission, Reihe C, Nr. 660, p. 126.

Auer, S., Hinz, S., Bamler, R., 2010. Ray-tracing simulation techniques for understanding high-resolution SAR images. IEEE Trans. Geosci. Remote Sens. 48 (3), 1445–1456.

Auer, S., Gernhardt, S., Bamler, R., 2011a. Ghost persistent scatterers related to multiple signal reflections. IEEE Geosci. Remote Sens. Lett. 8 (5), 919–923.

Auer, S., Gernhardt, S., Bamler, R., 2011b. Ghost persistent scatterers related to signal reflections between adjacent buildings. In: Proc. IGARSS 2011, Vancouver, Canada.

Balz, T., Stilla, U., 2009. Hybrid GPU-based single- and double-bounce SAR simulation. IEEE Trans. Geosci. Remote Sens. 47 (10), 3519–3529.

Brunner, D., Lemoine, G., Greidanus, H., Bruzzone, L., 2011. Radar imaging simulation for urban structures. IEEE Geosci. Remote Sens. Lett. 8 (1), 68–72.

Franceschetti, G., Migliaccio, M. Riccio, D., 1995. The SAR simulation: an overview. In: Proc. IGARSS'95, Florence, Italy, pp. 2283–2285.

Franceschetti, G., Iodice, A., Riccio, D., Ruello, G., 2003. SAR raw signal simulation for urban structures. IEEE Trans. Geosci. Remote Sens. 41 (9), 1986–1995.

Gelautz, M., Frick, H., Raggam, J., Burgstaller, J., Leberl, F., 1998. SAR image simulation and analysis of alpine terrain. ISPRS J. Photogrammetry Remote Sens. 53 (1), 17–38.

Gernhardt, S., Adam, N., Eineder, M., Bamler, R., 2010. Potential of very high resolution SAR for persistent scatterer interferometry in urban areas. Ann. GIS 16 (2), 103–111.

Hammer, H., Schulz, K., 2009. Coherent simulation of SAR images. Proc SPIE Image Signal Process. Remote Sens. XV 7477, pp. 74771K-1–8.

Hammer, H., Schulz, K., 2011. Dedicated SAR simulation tools for ATR and scene analysis. Proc. SPIE Image Anal. Model. Tech. XI 8179, pp. 81790N-1–9.

Stilla, U., 2007. High Resolution Radar Imaging of Urban Areas. In: Photogrammetric Week '07, Stuttgart, Germany, pp. 149–158.

Ulaby, F.T., Moore, R.K., Fung, A.K., 1986. Microwave Remote Sensing. vol. III, From Theory to Applications, London.

Xu, F., Jin, Y.Q., 2006. Imaging simulation of polarimetric SAR for a comprehensive terrain scene using the mapping and projection algorithm. IEEE Trans. Geosci. Remote Sens. 44 (11), 3219–3234.

Zhu, X., Bamler, R., 2010. Tomographic SAR inversion by L_1-norm regularization – the compressive sensing approach. IEEE Trans. Geosci. Remote Sens. 48 (10), 3839–3846.